MATCH
Communications in Mathematical and in Computer Chemistry

MATCH Commun. Math. Comput. Chem. **93** (2025) 267–290
ISSN: 0340–6253
doi: 10.46793/match.93-2.267C

Patterns of a General Chemical Model Involving Degn-Harrison Reaction Scheme

Mengxin Chen[a,*], **Junseok Kim**[b], **Seokjun Ham**[b]

a. College of Mathematics and Information Science, Henan Normal University, Xinxiang 453007, P. R. China

b. Department of Mathematics, Korea University, Seoul 02841, Republic of Korea

chmxdc@163.com

(Received March 24, 2024)

Abstract

This paper reports the pattern formation of a general Degn-Harrison system. We first determine the types and stability of the unique positive equilibrium for the spatially homogeneous system. The equilibrium may be node, focus, or center. Supercritical or subcritical Hopf bifurcation may occur if it is a center. In the sequel, we propose the conditions for the occurrence of Turing instability for the spatially inhomogeneous system. We can theoretically explain that Turing instability exists as the equilibrium transitions from homogeneous stable to inhomogeneous unstable states. Finally, we perform computational experiments to investigate the complex pattern formation of this chemical model. An interesting finding is that if one of the reactants has a high diffusion rate, the pattern formation will be inhibited. Conversely, a low diffusion rate may promote pattern formation.

1 Introduction

The reaction-diffusion equation is often used to qualitatively study various complex spatial and temporal dynamic phenomena, such as the evolution

*Corresponding author.

of biological populations, the spread of epidemic diseases, the control of chemical reactions, and so forth. One of the broadly investigated systems is the chemical model, which is governed by a couple of differential equations. It describes the mutual reactions among two or more reactants under certain conditions. Typical chemical reaction-diffusion systems include the Brusselator system [1,2], the Gierer-Meinhardt system [3,4], the Sel'kov-Schnakenberg system [5,6], the Degn-Harrison system [7,8], and other related chemical systems [9], etc.

The classic Degn-Harrison chemical system follows the reaction steps:

$$A \longrightarrow Y,\ B \Longleftrightarrow X,\ X + Y \longrightarrow P, \tag{1}$$

where X and Y are the concentrations of oxygen and nutrients, respectively. They are the intermediate reactants; A and B represent "sources," and their concentrations are set to be at a constant level. Moreover, they can be controlled in the reaction process; P is the final product of this reaction. The assumption is clear that the first and last steps are irreversible, while the second step is reversible [7]. Please refer to the original literature [8] for more details on this chemical reaction process. If the last step of the reaction process (1) follows the nonlinear rate equation of the form $XY/(1+\widetilde{q}X^2)$, where $\widetilde{q}$ is a constant, and it measures the strength of the inhibitory law, then one obtains the following reaction-diffusion equation based on this reaction process (1):

$$\begin{cases} \frac{\partial X}{\partial T} = D_1 \Delta X + a_2 B - a_3 X - \frac{a_4 XY}{1+\widetilde{q}X^2}, \\ \frac{\partial Y}{\partial T} = D_2 \Delta Y + a_1 A - \frac{a_4 XY}{1+\widetilde{q}X^2}, \end{cases} \tag{2}$$

where the constants D_1 and D_2 are diffusion rates of the reactants X and Y, respectively; positive constants a_1, a_2, a_3 and a_4 describe the reaction rate of the reactants; Δ is the classical Laplacian operator; T is time

variable. Now, consider the following dimensionless transformations [10]:

$$t = a_3 T,\ u = \frac{a_4}{a_3} X,\ v = \frac{a_4}{a_3} Y,\ a = \frac{a_2 a_4}{a_3^2} B,$$
$$b = \frac{a_1 a_4}{a_3^2} A,\ s = \frac{a_3^2}{a_4^2} \widetilde{q},\ d_1 = \frac{D_1}{a_3}, d_1 = \frac{D_2}{a_3}.$$

Then, the Degn-Harrison reaction system could be governed by:

$$\begin{cases} \frac{\partial u}{\partial t} = d_1 \Delta u + a - u - \frac{uv}{1+su^2}, \\ \frac{\partial v}{\partial t} = d_2 \Delta v + b - \frac{uv}{1+su^2}. \end{cases} \tag{3}$$

The Degn-Harrison reaction system (3) has attracted scholars for studying its various dynamic behaviors. Li et al. [7] reported the analytical properties of the nonconstant steady state and Turing patterns of the Degn-Harrison reaction system (3). Peng et al. [10] given the stability of the constant steady state, the nonexistence/existence of nonconstant steady state, the Hopf, and steady state bifurcations. Abbad et al. [11] investigated the local and global asymptotic stabilities of the system. By contracting the rectangles domain and the Lyapunov technique, Lisena [12] established sufficient conditions to ensure the global asymptotic stability of the positive equilibrium. Yan et al. [13] analyzed the existence of the Turing instability, Hopf bifurcation, and the direction of the Hopf bifurcation for the spatially inhomogeneous systems.

It is noticed that the reaction-diffusion Degn-Harrison system (3) is modeled by considering the nonlinear rate equation of the form $XY/(1 + \widetilde{q}X^2)$ in the last step of the reaction process (1). As a consequence, if taking the nonlinear rate equation $X^pY/(1 + \widetilde{q}X^q)$ (see also [14] for more general form) in the last step of the reaction process (1), one obtains the following reaction-diffusion equation with Degn-Harrison reaction scheme by involving the homogeneous zero-flux boundary conditions:

$$\begin{cases} \frac{\partial u}{\partial t} = d_1 \Delta u + a - u - \frac{Ku^p v}{1+su^q}, & x \in \Omega, \quad t > 0, \\ \frac{\partial v}{\partial t} = d_2 \Delta v + b - \frac{Ku^p v}{1+su^q}, & x \in \Omega, \quad t > 0, \\ \frac{\partial u}{\partial \nu} = \frac{\partial v}{\partial \nu} = 0, & x \in \partial\Omega, \quad t \geq 0, \\ u(x,0) = u_0(x) \geq 0, \quad v(x,0) = v_0(x) \geq 0, & x \in \Omega, \end{cases} \tag{4}$$

where we suppose that $\Omega \subset \mathbb{R}^N$ is a bounded domain with $N \geq 1$; $\frac{\partial u}{\partial \nu} = \frac{\partial v}{\partial \nu} = 0$ is the zero-flux boundary condition and it suggests that the chemical model (4) is a closed system; ν is the outward unit normal vector along the smooth boundary $\partial\Omega$; $u_0(x) \geq 0$ and $v_0(x) \geq 0$ are the initial concentrations of two reactants u and v, respectively; K, p, and q are positive constants. Obviously, if one chooses $K = 1, p = 1$, and $q = 2$, then chemical system (4) degenerates into system (3). Therefore, chemical system (4) is a general Degn-Harrison chemical reaction system.

As it is well known, pattern formation is a vital aspect of figuring out the complex spatiotemporal dynamic behaviors of the reaction-diffusion systems. It may be induced by the Turing instability due to the diffusion effect, for example, the self-diffusion and cross-diffusion. Nowadays, there are many existing literature that have reported the pattern formation for various reaction-diffusion systems, such as the population systems [15–19], the chemical systems [2, 4, 20–22], the epidemic propagation systems [23–25], and so on. However, we noticed that few scholars have studied the spatial pattern formation phenomenon of the aforementioned general Degn-Harrison chemical reaction system (4). In this paper, we are interested in studying the pattern dynamics of the system (4). When $0 < b < a$, the system admits a unique positive equilibrium $E_* = (u_*, v_*)$. Furthermore, we can show that it is a node or focus or center as the positive constant p, q satisfy $p \geq q$ or $\frac{squ_*^q}{su_*^q+1} - \frac{u_*}{b} \leq p < q$ or $0 < p < \frac{squ_*^q}{su_*^q+1} - \frac{u_*}{b}$ and $q > \frac{su_*^q+1}{bsu_*^{q-1}}$. If equilibrium E_* is the center, there is the homogeneous Hopf bifurcation when treating K as the bifurcation parameter. We also theoretically explain that system (4) undergoes the Turing instability when restricting $0 < p < \frac{squ_*^q}{su_*^q+1} - \frac{u_*}{b}$ and $q > \frac{su_*^q+1}{bsu_*^{q-1}}$. In this fashion, the complex pattern dynamics can be displayed by using numerical simulations. Precisely, the general Degn-Harrison system (4) enjoys patterns in one-dimensional space, two-dimensional space, on a torus surface, and on a spherical surface. These results sufficiently illustrate that the general Degn-Harrison system (4) has wealth and complex dynamic profiles.

This paper is structured as follows. In Sec. 2, we investigate the local linear stability of the unique positive equilibrium of the local spatially homogenous system. In Sec. 3, we establish the conditions to ensure

the existence for the Turing instability in the spatial diffusive system. In Sec. 4, the spatial pattern formation is displayed by using numerical experiments. Finally, this paper ends with brief summary made in Sec. 5.

2 Stability for the local system

Now, let us explore the Hopf bifurcation of the spatially homogeneous system. Consider the following local system:

$$\begin{cases} \frac{du}{dt} = a - u - \frac{Ku^p v}{1+su^q}, \\ \frac{dv}{dt} = b - \frac{Ku^p v}{1+su^q}. \end{cases} \tag{5}$$

Define $f(u,v) := a - u - \frac{Ku^p v}{1+su^q}$ and $g(u,v) := b - \frac{Ku^p v}{1+su^q}$. By direct calculation, the local system (5) possesses a unique positive equilibrium $E_* = (u_*, v_*) = \left(a-b, \frac{b[1+s(a-b)^q]}{K(a-b)^p}\right)$ with $0 < b < a$ if letting $f(u,v) = g(u,v) = 0$. As a consequence, the Jacobian matrix, denoted by J_0, at the unique positive equilibrium $E_* = (u_*, v_*)$ takes the form

$$J_0 = \begin{pmatrix} -1 - \frac{b[s(p-q)u_*^q + p]}{u_*(su_*^q+1)} & -\frac{Ku_*^p}{1+su_*^q} \\ -\frac{b[s(p-q)u_*^q+p]}{u_*(su_*^q+1)} & -\frac{Ku_*^p}{1+su_*^q} \end{pmatrix}.$$

Therefore, we obtain the characteristic equation at $E_* = (u_*, v_*)$ as follows

$$\lambda^2 - T_0(K)\lambda + D_0(K) = 0, \tag{6}$$

where $T_0(K) = -\frac{b[s(p-q)u_*^q+p]}{u_*(su_*^q+1)} - \frac{Ku_*^p}{1+su_*^q} - 1$ and $D_0(K) = \frac{Ku_*^p}{1+su_*^q} > 0$. By solving the eigenvalue λ from (6), one gets

$$\lambda = \frac{T_0(K) \pm \sqrt{T_0^2(K) - 4D_0(K)}}{2}.$$

In order to facilitate theoretical analysis, we set $\widetilde{K} = \frac{b[s(p-q)u_*^q+p]}{u_*(su_*^q+1)} + 1$ and $\widehat{K} = \frac{u_*^p}{1+su_*^q}$. These indicate that $T_0(K) = -\widehat{K}K - \widetilde{K}$ and $D_0(K) = \widehat{K}K > 0$. Obviously, $\widehat{K} > 0$ while the sign of $\widetilde{K}$ could be given by the following.

Proposition 1. *Suppose that $0 < b < a$ is valid.*

(i) If $p \geq q$, then $\widetilde{K} > 1$;

(ii) If $\frac{squ_*^q}{su_*^q+1} \le p < q$, *then* $\widetilde{K} \ge 1$;

(iii) If $\frac{squ_*^q}{su_*^q+1} - \frac{u_*}{b} \le p < \frac{squ_*^q}{su_*^q+1}$, *then* $0 < \widetilde{K} < 1$;

(iv) If $0 < p < \frac{squ_*^q}{su_*^q+1} - \frac{u_*}{b}$ *and* $q > \frac{su_*^q+1}{bsu_*^{q-1}}$, *then* $\widetilde{K} < 0$.

Proof. It is noticed that $\widetilde{K} = \frac{b[s(p-q)u_*^q+p]}{u_*(su_*^q+1)} + 1$, if $p \ge q$, we have $\widetilde{K} = \frac{b[s(p-q)u_*^q+p]}{u_*(su_*^q+1)} + 1 \ge \frac{bp}{u_*(su_*^q+1)} + 1 \ge 1$. (i) is valid. If $\frac{squ_*^q}{su_*^q+1} \le p < q$, then $\widetilde{K} = \frac{b[s(p-q)u_*^q+p]}{u_*(su_*^q+1)} + 1 \ge 1$. (ii) is true. For (iii), if $\frac{squ_*^q}{su_*^q+1} - \frac{u_*}{b} \le p < \frac{squ_*^q}{su_*^q+1}$, one immediately obtains $\frac{b[s(p-q)u_*^q+p]}{u_*(su_*^q+1)} < 0$ while $\frac{b[s(p-q)u_*^q+p]}{u_*(su_*^q+1)} + 1 > 0$. These give that $0 < \widetilde{K} < 1$. Finally, (iv) is a direct consequence by using the condition $0 < p < \frac{squ_*^q}{su_*^q+1} - \frac{u_*}{b}$ and $q > \frac{su_*^q+1}{bsu_*^{q-1}}$. This ends the proof.

In what follows, letting $H(K) := T_0^2(K) - 4D_0(K)$. This is

$$H(K) = \widehat{K}^2K^2 + 2\widehat{K}(\widetilde{K} - 2)K + \widetilde{K}^2.$$

Benefiting from Proposition 1, we insert the following result.

Proposition 2. *Suppose that* $0 < b < a$ *is valid.*

(i) If $p \ge q$ *or* $\frac{squ_*^q}{su_*^q+1} < p < q$, *then* $H(K) = 0$ *has no real roots;*

(ii) If $\frac{squ_*^q}{su_*^q+1} = p < q$, *then* $H(K) = 0$ *has a unique positive real solution* $K_1 = \frac{1}{\widetilde{K}}$;

(iii) If $0 < p < \frac{squ_*^q}{su_*^q+1}$, *then* $H(K) = 0$ *has two different positive solutions*

$$K_2 = \frac{2 - \widetilde{K} - 2\sqrt{1-\widetilde{K}}}{\widehat{K}}, \quad K_3 = \frac{2 - \widetilde{K} + 2\sqrt{1-\widetilde{K}}}{\widehat{K}}.$$

Proof. To discuss the root's existence of $H(K) = 0$, let us first perform the root's existence discriminant, denote by $\Delta_{H(K)}$ of $H(K) = 0$, where $\Delta_{H(K)} = 16\widehat{K}^2(1 - \widetilde{K})$. Now, if $p \ge q$ or $\frac{squ_*^q}{su_*^q+1} < p < q$ is satisfied, then using Proposition 1, we can infer that $\widetilde{K} > 1$ always holds. We immediately have $\Delta_{H(K)} = 16\widehat{K}^2(1 - \widetilde{K}) < 0$, so (i) holds. When $\frac{squ_*^q}{su_*^q+1} = p < q$ in (ii) is true, we can yield $\widetilde{K} = 1$. This is $\Delta_{H(K)} = 16\widehat{K}^2(1 - \widetilde{K}) = 0$. As such, $H(K) = 0$ has a unique positive real solution $K_1 = \frac{1}{\widetilde{K}}$. Now, if $0 < p < \frac{squ_*^q}{su_*^q+1}$, then we know that there must holds $0 < \widetilde{K} < 1$ or $\widetilde{K} \le 0$, see (iii) and (iv) in Proposition 1. Therefore, one yields $\Delta_{H(K)} = 16\widehat{K}^2(1-\widetilde{K}) > 0$ and $\widetilde{K} - 2 < 0$. Hence, (iii) is valid. This ends the proof.

Proposition 3. *Suppose that* $0 < b < a$ *is valid.*

(i) If $p \geq q$ *or* $\frac{squ_*^q}{su_*^q+1} \leq p < q$, *then* $H(K) \geq 0$;

(ii) If $0 < p < \frac{squ_*^q}{su_*^q+1}$, *then* $H(K) \geq 0$ *when* $0 < K \leq K_2$ *or* $K \geq K_3$; *moreover,* $H(K) < 0$ *when* $K_2 < K < K_3$.

Proof. (i) and (ii) can be directly obtained by using Proposition 2.

Now, we establish the following stability result about E_*.

Theorem 1. *Suppose that* $0 < b < a$ *is valid.*

(i) If $p \geq q$ *or* $\frac{squ_*^q}{su_*^q+1} - \frac{u_*}{b} \leq p < q$, *then* E_* *is a stable node;*

(ii) If $0 < p < \frac{squ_*^q}{su_*^q+1} - \frac{u_*}{b}$ *and* $K \geq K_3$, *then* E_* *is a stable node; also, if* $0 < K \leq K_2$, *then* E_* *is a unstable node;*

(iii) If $0 < p < \frac{squ_*^q}{su_*^q+1} - \frac{u_*}{b}$ *and* $-\frac{\widetilde{K}}{\widehat{K}} < K < K_3$, *then* E_* *is a stable focus; if* $K_2 < K < -\frac{\widetilde{K}}{\widehat{K}}$, *then* E_* *is a unstable focus;*

(iv) If $0 < p < \frac{squ_*^q}{su_*^q+1} - \frac{u_*}{b}$, $q > \frac{su_*^q+1}{bsu_*^{q-1}}$, *and* $K = -\frac{\widetilde{K}}{\widehat{K}}$, *then* E_* *is a center.*

Proof. Owing to $T_0(K) = -\widehat{K}K - \widetilde{K}$ and $D_0(K) = \widehat{K}K > 0$. Thereby, the stability of the equilibrium E_* is uniquely determined by the sign of $T_0(K)$. If $p \geq q$ or $\frac{squ_*^q}{su_*^q+1} - \frac{u_*}{b} \leq p < q$ is satisfied in (i), then by using (i)-(iii) of Proposition 1, we can deduce that $\widetilde{K} \geq 0$ holds. Accordingly, we have $T_0(K) = -\widehat{K}K - \widetilde{K} < 0$. So E_* is a stable node.

For (ii), the condition $0 < p < \frac{squ_*^q}{su_*^q+1} - \frac{u_*}{b}$ means that $\widetilde{K} < 0$ due to (iv) of Proposition 1. Also, if $K \geq K_3$ is valid, one has $H(K) \geq 0$ by using (ii) of Proposition 3 and $T_0(K) = -\widehat{K}K - \widetilde{K} \leq -\widehat{K}K_3 - \widetilde{K} = -2 - 2\sqrt{1-\widetilde{K}} < 0$. As a consequence, E_* is a stable node. Now, if $0 < K \leq K_2$, then $T_0(K) = -\widehat{K}K - \widetilde{K} \geq -\widehat{K}K_2 - \widetilde{K} = -2 + 2\sqrt{1-\widetilde{K}} > 0$. For this case, E_* is an unstable node.

For (iii), if $0 < p < \frac{squ_*^q}{su_*^q+1} - \frac{u_*}{b}$, then we have $\widetilde{K} < 0$ by using Proposition 1. In addition, if $-\frac{\widetilde{K}}{\widehat{K}} < K < K_3$, one has $T_0(K) = -\widehat{K}K - \widetilde{K} < \widetilde{K} - \widetilde{K} = 0$ and $K_2 < -\frac{\widetilde{K}}{\widehat{K}} < K < K_3$. This implies that $H(K) < 0$ by using (ii) of Proposition 3. To sum up, it can be seen that E_* is a stable focus. Similarly, we can show that E_* is an unstable focus.

Finally, if $0 < p < \frac{squ_*^q}{su_*^q+1} - \frac{u_*}{b}$ and $K = -\frac{\widetilde{K}}{\widehat{K}}$, one can get $\widetilde{K} < 0$ by using Proposition 1 and $H(K) < 0$ by using (ii) of Proposition 3 since

$0 < p < \frac{squ_*^q}{su_*^q+1} - \frac{u_*}{b} < \frac{squ_*^q}{su_*^q+1}$ and $K_2 < -\frac{\widetilde{K}}{\widehat{K}} < K < K_3$. This implies that E_* is a center. We finish the proof.

Example 1. Let us perform some numerical experiments to show the validity of Theorem 1.

(I) Taking $a = 1.5, b = 0.5, p = 2, q = 1, K = 0.65, s = 0.45$, then we can obtain $E_* = (1, 1.1154)$. Obviously, we have $p > q$ and equilibrium $E_* = (1, 1.1154)$ is a stable node, as shown in Fig. 1(a).

(II) We shall choose $a = 1.45, b = 0.5, p = 2, q = 3, K = 0.65, s = 0.45$, then one has $E_* = (0.95, 1.1812)$ and $-1.0648 = \frac{squ_*^q}{su_*^q+1} - \frac{u_*}{b} < p < q$. It is found that $E_* = (0.95, 1.1812)$ is a stable node, see Fig. 1(b).

(III) Let us take $a = 1.75, b = 0.5, p = 1, q = 6, K = 10.65, s = 0.45$, then one has $E_* = (1.25, 0.102)$, $\frac{squ_*^q}{su_*^q+1} - \frac{u_*}{b} = 1.2914, K_2 = 0.007$, and $K_3 = 9.1928$. Accordingly, all conditions in (ii) are satisfied, then our computational experiment shows that $E_* = (1.25, 0.102)$ is a stable node, as shown in Fig. 1(c).

(IV) Now, we treat the specific parameter values: $a = 1.75, b = 0.5, p = 1, q = 6, K = 2, s = 0.45$, then one has $E_* = (1.25, 0.5433)$, $\frac{squ_*^q}{su_*^q+1} - \frac{u_*}{b} = 1.2914, -\frac{\widetilde{K}}{\widehat{K}} = 0.2533, K_2 = 0.007$, and $K_3 = 9.1928$. In this manner, all conditions in (iii) are satisfied. Thus, our numerical experiment shows that $E_* = (1.25, 0.5433)$ is a stable focus, as seen in Fig. 1(d).

When $0 < p < \frac{squ_*^q}{su_*^q+1} - \frac{u_*}{b}$, $q > \frac{su_*^q+1}{bsu_*^{q-1}}$ and $K = -\frac{\widetilde{K}}{\widehat{K}}$, (iv) of Theorem 1 shows that E_* is a center. Thereby, a Hopf bifurcation may exist. The following result can confirm this prediction.

Theorem 2. *Suppose that $0 < b < a$ is valid. If $0 < p < \frac{squ_*^q}{su_*^q+1} - \frac{u_*}{b}$, $q > \frac{su_*^q+1}{bsu_*^{q-1}}$, and $K = -\frac{\widetilde{K}}{\widehat{K}}$, then model (5) has the Hopf bifurcation. Moreover, the direction of the Hopf bifurcation could be determined by the first Lyapunov number L_1, which will be presented later.*

Proof. Obviously, $\widetilde{K} < 0$ because of $0 < p < \frac{squ_*^q}{su_*^q+1} - \frac{u_*}{b}$ and $q > \frac{su_*^q+1}{bsu_*^{q-1}}$. Therefore, we claim that $K = -\frac{\widetilde{K}}{\widehat{K}} > 0$. We immediately get $T_0(K) = -\widehat{K}K - \widetilde{K} = 0$ as $K = -\frac{\widetilde{K}}{\widehat{K}}$, and thereby, the characteristic equation (6) possesses a pair of purely imaginary roots. One can also

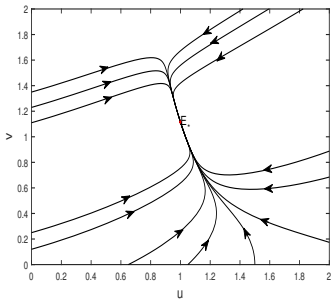

(a) $a = 1.5, b = 0.5, p = 2, q = 1, K = 0.65, s = 0.45$

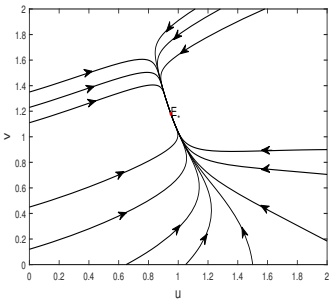

(b) $a = 1.45, b = 0.5, p = 2, q = 3, K = 0.65, s = 0.45$

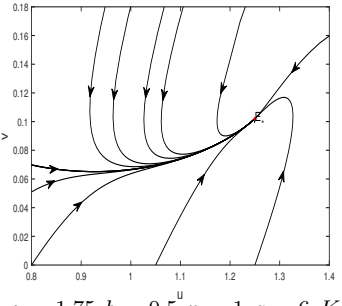

(c) $a = 1.75, b = 0.5, p = 1, q = 6, K = 10.65, s = 0.45$

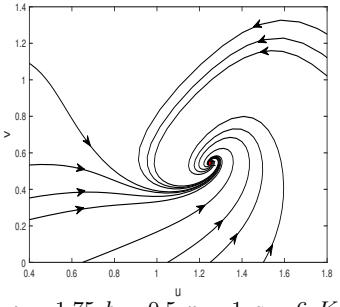

(d) $a = 1.75, b = 0.5, p = 1, q = 6, K = 2, s = 0.45$

Figure 1. Plane phase diagrams of the system (5). (a): $E_* = (1, 1.1154)$ is a stable node; (b): $E_* = (0.95, 1.1812)$ is a stable node; (c): $E_* = (1.25, 0.102)$ is a stable node; (d): $E_* = (1.25, 0.5433)$ is a stable focus.

calculate that

$$\frac{d}{dK} Re\{\lambda\}\Big|_{K=-\frac{\widetilde{K}}{\widehat{K}}} = \frac{1}{2}\frac{d}{dK} T_0(K)\Big|_{K=-\frac{\widetilde{K}}{\widehat{K}}} = -\frac{\widehat{K}}{2} < 0.$$

As a result, the Poincaré Andronov-Hopf bifurcation theory guarantees that system (5) undergoes the Hopf bifurcation.

In the sequel, let $\check{u} = u - u_*, \check{v} = v - v_*$ and denote $\check{u}, \check{v}$ by u, v,

respectively. Then, system (5) takes the form:

$$\begin{cases} \frac{du}{dt} = & \delta_{10}u + \delta_{01}v + \delta_{20}u^2 + \delta_{11}uv + \delta_{02}v^2 + \delta_{30}u^3 + \delta_{21}u^2v \\ & +\delta_{12}uv^2 + \delta_{03}v^3 + \mathcal{O}(|u,v|^4), \\ \frac{dv}{dt} = & \eta_{10}u + \eta_{01}v + \eta_{20}u^2 + \eta_{11}uv + \eta_{02}v^2 + \eta_{30}u^3 + \eta_{21}u^2v \\ & +\eta_{12}uv^2 + \eta_{03}v^3 + \mathcal{O}(|u,v|^4), \end{cases} \tag{7}$$

where $\mathcal{O}(|u,v|^4)$ are higher terms and

$$\begin{aligned}
\delta_{10} =& -\frac{Kv_*u_*^{p-1}[s(p-q)u_*^q+p]}{(su_*^q+1)^2} - 1, \quad \delta_{01} = -\frac{Ku_*^p}{1+su_*^q}, \\
\delta_{20} =& -Kv_*u_*^p\left[\frac{q^2s^2u^{2q-2}}{(su_*^q+1)^3} - \frac{q(q-1)su_*^{q-2}}{2(su_*^q+1)^2}\right] - \frac{K(p-1)pv_*u_*^{p-2}}{2(su_*^q+1)} \\
& + \frac{Kpqsv_*u_*^{p+q-2}}{(su_*^q+1)^2}, \\
\delta_{11} =& -\frac{Ku_*^{p-1}(psu_*^q+p-qsu_*^q)}{(su_*^q+1)^2}, \quad \delta_{02} = \delta_{12} = \delta_{03} = 0, \\
\delta_{30} =& -Kpv_*u^{p-1}\left[\frac{q^2s^2u_*^{2q-2}}{(su_*^q+1)^3} - \frac{q(q-1)su_*^{q-2}}{2(su_*^q+1)^2}\right] \\
& - Kvu_*^p\left[-\frac{q^3s^3u_*^{3q-3}}{(su_*^q+1)^4} + \frac{q^2(q-1)s^2u_*^{2q-3}}{(su_*^q+1)^3} - \frac{(q-2)(q-1)qsu_*^{q-3}}{6(su_*^q+1)^2}\right] \\
& - \frac{K(p-2)(p-1)pv_*u_*^{p-3}}{6(su_*^q+1)} + \frac{K(p-1)pqsvu^{p+q-3}}{2(su_*^q+1)^2}, \\
\delta_{21} =& -\frac{Kq^2s^2u_*^{p+2q-2}}{2(su_*^q+1)^3} + \frac{Kqs(q-1+2p)u_*^{p+q-2}}{2(su_*^q+1)^2} + \frac{Kp(1-p)u_*^{p-2}}{2(su_*^q+1)}, \\
\eta_{10} =& -\frac{Kv_*u_*^{p-1}[s(p-q)u_*^q+p]}{(su_*^q+1)^2}, \quad \eta_{01} = -\frac{Ku_*^p}{1+su_*^q}, \\
\eta_{20} =& -Kv_*u_*^p\left[\frac{q^2s^2u_*^{2q-2}}{(su_*^q+1)^3} - \frac{q(q-1)su_*^{q-2}}{2(su_*^q+1)^2}\right] - \frac{K(p-1)pv_*u_*^{p-2}}{2(su_*^q+1)} \\
& + \frac{Kpqsv_*u_*^{p+q-2}}{(su_*^q+1)^2}, \\
\eta_{11} =& -\frac{Ku_*^{p-1}(psu_*^q+p-qsu_*^q)}{(su_*^q+1)^2}, \quad \eta_{02} = \eta_{12} = \eta_{03} = 0,
\end{aligned}$$

$$\begin{aligned}
\eta_{30} =& - Kpv_*u_*^{p-1}\left[\frac{q^2s^2u_*^{2q-2}}{(su_*^q+1)^3} - \frac{q(q-1)su_*^{q-2}}{2(su_*^q+1)^2}\right] \\
& - Kv_*u_*^p\left[-\frac{q^3s^3u^{3q-3}}{(su_*^q+1)^4} + \frac{q^2(q-1)s^2u_*^{2q-3}}{(su_*^q+1)^3} - \frac{(q-2)(q-1)qsu_*^{q-3}}{6(su_*^q+1)^2}\right] \\
& - \frac{K(p-2)(p-1)pv_*u_*^{p-3}}{6(su_*^q+1)} + \frac{K(p-1)pqsvu^{p+q-3}}{2(su_*^q+1)^2}, \\
\eta_{21} =& - \frac{Kq^2s^2u_*^{p+2q-2}}{2(su_*^q+1)^3} + \frac{Kqs(q-1+2p)u_*^{p+q-2}}{2(su_*^q+1)^2} + \frac{Kp(1-p)u_*^{p-2}}{2(su_*^q+1)}.
\end{aligned}$$

Consequently, the first Lyapunov number can be expressed as follows:

$$\begin{aligned}
L_1 =& \frac{-3\pi}{2\delta_{01}\mathrm{D}_0(K)^{3/2}}\{[\delta_{10}\eta_{10}(\delta_{11}^2 + \delta_{11}\eta_{02} + \delta_{02}\eta_{11}) \\
& + \delta_{10}\delta_{01}(\eta_{11}^2 + \delta_{20}\eta_{11} + \delta_{11}\eta_{02}) + \eta_{10}^2(\delta_{11}\delta_{02} + 2\delta_{02}\eta_{02}) \\
& - 2\delta_{10}\eta_{10}(\eta_{02}^2 - \delta_{20}\delta_{02}) - 2\delta_{10}\delta_{01}(\delta_{20}^2 - \eta_{20}\eta_{02}) \\
& - \delta_{01}^2(2\eta_{20}\delta_{20} + \eta_{11}\eta_{20}) + (\delta_{01}\eta_{10} - 2\delta_{10}^2)(\eta_{11}\eta_{02} - \delta_{11}\delta_{20})] \\
& - (\delta_{10}^2 + \delta_{01}\eta_{10})[3(\eta_{10}\eta_{03} - \delta_{01}\delta_{30}) + 2\delta_{10}(\delta_{21} + \eta_{12}) \\
& + (\eta_{10}\delta_{12} - \delta_{01}\eta_{21})]\} \\
=& \frac{-3\pi}{2\delta_{01}\mathrm{D}_0(K)^{3/2}}\{[\delta_{10}\eta_{10}\delta_{11}^2 + \delta_{10}\delta_{01}(\eta_{11}^2 + \delta_{20}\eta_{11}) - 2\delta_{10}\delta_{01}\delta_{20}^2 \\
& - \delta_{01}^2(2\eta_{20}\delta_{20} + \eta_{11}\eta_{20}) - (\delta_{01}\eta_{10} - 2\delta_{10}^2)\delta_{11}\delta_{20}] \\
& - (\delta_{10}^2 + \delta_{01}\eta_{10})(-3\delta_{01}\delta_{30} + 2\delta_{10}\delta_{21} - \delta_{01}\eta_{21})\}.
\end{aligned}$$

Based on [26], we know that the Hopf bifurcation is supercritical when $L_1 < 0$ and it is subcritical when $L_1 > 0$. The proof is completed.

Example 2.

(I) Fixing the parameters $a = 1.75, b1 = 0.5, p = 3, q = 8, s = 0.45$, then we can derive $\frac{squ_*^q}{su_*^q+1} - \frac{u_*}{b} = 3.3274$ and $-\frac{\widetilde{K}}{\widehat{K}} = 0.2469$. Therefore, if one chooses $K = 0.2469$, then the conditions $0 < p < \frac{squ_*^q}{su_*^q+1} - \frac{u_*}{b}$ and $K = -\frac{\widetilde{K}}{\widehat{K}}$ in Theorem 2 are satisfied. In this fashion, we can obtain $E_* = (1.25, 3.8179)$ and the following facts

$$\begin{gathered}
\delta_{10} = 0.1310,\ \delta_{01} = -0.1310,\ \delta_{20} = 0.2943,\ \delta_{11} = 0.2962, \\
\delta_{30} = -5.9479,\ \delta_{21} = 1.5002,\ \eta_{10} = 1.1310,\ \eta_{01} = -0.1310, \\
\eta_{20} = 0.2943,\ \eta_{11} = 0.2962,\ \ \eta_{30} = -5.9479,\ \eta_{21} = 1.5002.
\end{gathered}$$

Hence, we can compute the first Lyapunov number $L_1 = -155.2266 < 0$. By employing Theorem 2, we know that the spatially homogeneous system (5) undergoes the supercritical Hopf bifurcation. This prediction is also confirmed by our computational experiment, see Fig. 2 (a). It is found that there are stable periodic solutions due to the supercritical Hopf bifurcation.

(II) Choosing $a = 1.5, b1 = 0.5, p = 1, q = 9, s = 0.75$, then we have $\frac{squ_*^q}{su_*^q+1} - \frac{u_*}{b} = 1.8571$ and $-\frac{\widetilde{K}}{\widehat{K}} = 0.75$. Now, one takes $K = 0.75$, then the assumptions in Theorem 2 are satisfied. In addition, we can obtain $E_* = (1, 1.1667)$ and

$$\begin{gathered}\delta_{10} = 0.4286,\ \delta_{01} = -0.4286,\ \delta_{20} = 2.2041,\ \delta_{11} = 1.2245,\\ \delta_{30} = -12.5423,\ \delta_{21} = 5.0773,\ \eta_{10} = 1.4286,\ \eta_{01} = -0.4286,\\ \eta_{20} = 2.2041,\ \eta_{11} = 1.2245,\ \ \eta_{30} = -12.5423,\ \eta_{21} = 5.0773.\end{gathered}$$

As a consequence, we can compute the first Lyapunov number $L_1 = -71.2649 < 0$. By employing Theorem 2, we know that the spatially homogeneous system (5) undergoes the supercritical Hopf bifurcation and there are stable periodic solutions, see Fig. 2 (b).

3 Turing instability for the diffusive system

To obtain the emergence condition of the Turing instability of the diffusive system, let us first consider the linearization system of (4) at the unique positive equilibrium E_*. This is

$$\begin{cases} \frac{\partial u}{\partial t} \approx d_1\Delta u - \widetilde{K}u - K\widehat{K}v, & x \in \Omega,\ \ t > 0,\\ \frac{\partial v}{\partial t} \approx d_2\Delta v + (1-\widetilde{K})u - K\widehat{K}v, & x \in \Omega,\ \ t > 0,\\ \frac{\partial u}{\partial \nu} = \frac{\partial v}{\partial \nu} = 0, & x \in \partial\Omega,\ \ t \geq 0,\\ u(x,0) = u_0(x) \geq 0,\ \ v(x,0) = v_0(x) \geq 0, & x \in \Omega, \end{cases} \tag{8}$$

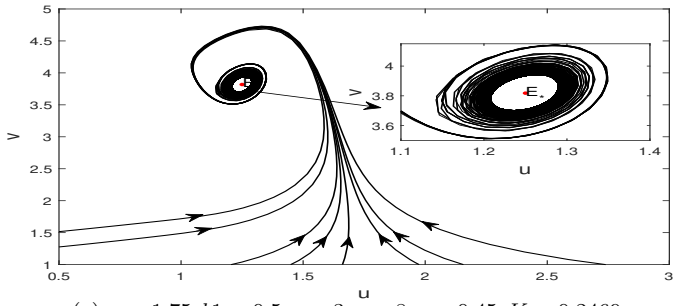

(a) $a = 1.75, b1 = 0.5, p = 3, q = 8, s = 0.45, K = 0.2469$

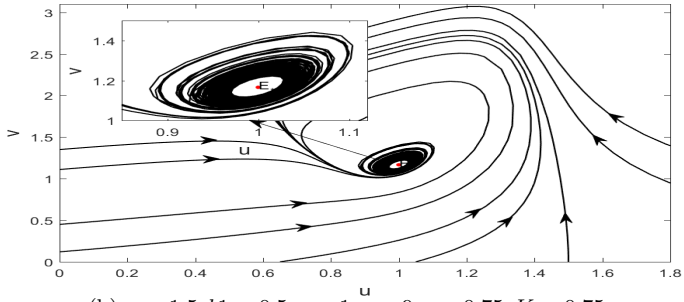

(b) $a = 1.5, b1 = 0.5, p = 1, q = 9, s = 0.75, K = 0.75$

Figure 2. Spatially homogeneous system (5) undergoes the supercritical Hopf bifurcation and there are stable periodic solutions.

where $\widetilde{K} = \frac{b[s(p-q)u_*^q + p]}{u_*(su_*^q + 1)} + 1$ and $\widehat{K} = \frac{u_*^p}{1+su_*^q}$. As such, system (8) can be expressed as follows:

$$\begin{pmatrix} \frac{\partial u}{\partial t} \\ \frac{\partial v}{\partial t} \end{pmatrix} = L \begin{pmatrix} u \\ v \end{pmatrix} = D \begin{pmatrix} u \\ v \end{pmatrix} + J_0 \begin{pmatrix} u \\ v \end{pmatrix}, \tag{9}$$

where

$$D = \begin{pmatrix} d_1\Delta & 0 \\ 0 & d_2\Delta \end{pmatrix}, \quad J_0 = \begin{pmatrix} -\widetilde{K} & -K\widehat{K} \\ 1-\widetilde{K} & -K\widehat{K} \end{pmatrix}.$$

For system (9), let us consider the following eigenvalue problem

$$L\begin{pmatrix}\Omega_1\\ \Omega_2\end{pmatrix}=\lambda_k\begin{pmatrix}\Omega_1\\ \Omega_2\end{pmatrix},\quad k\in\mathbb{N}_0=\{0,1,2,\cdots\}$$

with

$$\begin{pmatrix}\Omega_1\\ \Omega_2\end{pmatrix}=\sum_{k=0}^{\infty}\begin{pmatrix}\alpha_k\\ \beta_k\end{pmatrix}e^{\lambda_k t}\cos(kx),$$

where we assume that α_k,β_k are constants. As a result, one has

$$\sum_{k=0}^{\infty}(J_k-\lambda_k I)\begin{pmatrix}\alpha_k\\ \beta_k\end{pmatrix}e^{\lambda_k t}\cos(kx)=0,$$

where

$$J_k=\begin{pmatrix}-\widetilde{K}-d_1k^2 & -K\widehat{K}\\ 1-\widetilde{K} & -K\widehat{K}-d_2k^2\end{pmatrix}.$$

Hence, we can obtain the characteristic equation for the diffusive system as follows:

$$\lambda_k^2-T_k(K)\lambda_k+D_k(K)=0, \tag{10}$$

where

$$\begin{cases}T_k(K)=-(d_1+d_2)k^2-K\widehat{K}-\widetilde{K},\\ D_k(K)=d_1d_2k^4+(d_2\widetilde{K}+d_1K\widehat{K})k^2+K\widehat{K}.\end{cases}$$

To ensure the existence of the Turing instability for the diffusive model (4), the first step is to guarantee the local asymptotic stability of the positive equilibrium E_* for the spatially homogeneous system (5), while it loses its local asymptotic stability for the spatially inhomogeneous system (4). In the following, we always assume that $0<p<\frac{squ_*^q}{su_*^q+1}-\frac{u_*}{b}$, $q>\frac{su_*^q+1}{bsu_*^{q-1}}$, and $K>-\frac{\widetilde{K}}{\widehat{K}}$ are true to ensure the positive equilibrium E_* is locally asymptotically stable for the spatially homogeneous system (5).

Keeping these conditions in mind, we state the following theorem:

Theorem 3. *Suppose that* $0 < b < a, 0 < p < \frac{squ_*^q}{su_*^q+1} - \frac{u_*}{b}$, *and* $q > \frac{su_*^q+1}{bsu_*^{q-1}}$ *are valid. For the general Degn-Harrison system (4),*

(i) if $d_2 \geq d_1$ *and* $K \geq -\frac{d_2\widetilde{K}}{d_1\widehat{K}}$, *then* E_* *is stable;*

(ii) if $d_2 < d_1$ *and* $K \geq -\frac{\widetilde{K}}{\widehat{K}}$, *then* E_* *is stable;*

(iii) if $\max\left\{K_1^*, -\frac{\widetilde{K}}{\widehat{K}}\right\} < K < -\frac{d_2\widetilde{K}}{d_1\widehat{K}}$, *then* E_* *is stable;*

(iv) if $-\frac{\widetilde{K}}{\widehat{K}} < K < K_1^*$, *then* E_* *is unstable and system (4) suffers from the Turing instability, where*

$$K_1^* = \frac{d_2}{d_1}K_2 > 0, \quad K_2^* = \frac{d_2}{d_1}K_3 > 0,$$

with

$$K_2 = \frac{2 - \widetilde{K} - 2\sqrt{1-\widetilde{K}}}{\widehat{K}}, \quad K_3 = \frac{2 - \widetilde{K} + 2\sqrt{1-\widetilde{K}}}{\widehat{K}}.$$

Proof. Since we require that $K > -\frac{\widetilde{K}}{\widehat{K}}$, one observe that $T_k(K) = -(d_1+d_2)k^2 - K\widehat{K} - \widetilde{K} < 0$ always holds for any $k \in \mathbb{N}_0$. This means that we should only focus on the sign of $D_k(K)$ to analyze the stability of the equilibrium E_*. Obviously, if $K \geq -\frac{d_2\widetilde{K}}{d_1\widehat{K}}$ is valid, then we can ensure that $D_k(K) = d_1d_2k^4 + (d_2\widetilde{K} + d_1K\widehat{K})k^2 + K\widehat{K} \geq d_1d_2k^4 + K\widehat{K} > 0$. This implies that the equilibrium E_* is locally asymptotically stable. Therefore, the parameter K should satisfy $K > \max\left\{-\frac{\widetilde{K}}{\widehat{K}}, -\frac{d_2\widetilde{K}}{d_1\widehat{K}}\right\}$. This indicates that conditions (i) and (ii) are true.

In the sequel, let us assume that $d_2\widetilde{K} + d_1K\widehat{K} < 0$, namely, one requires that $K < -\frac{d_2\widetilde{K}}{d_1\widehat{K}}$. Treating K as the potential critical parameter of the Turing instability and considering the critical instability case, $\min_{k\in\mathbb{N}_0\setminus\{0\}} D_k(K) = 0$. Then we can compute that $\min_{k\in\mathbb{N}_0\setminus\{0\}} D_k(K) := -\phi(K) = 0$, where

$$\phi(K) = d_1^2\widehat{K}^2K^2 + 2d_1d_2\widehat{K}(\widetilde{K} - 2)K + d_2^2\widetilde{K}^2.$$

It is noticed that $\widetilde{K} < 0$ as $0 < p < \frac{squ_*^q}{su_*^q+1} - \frac{u_*}{b}$ (see (iv) of Proposition 1). Therefore, $\phi(K) = 0$ must have two different positive real roots, denoted

by K_1^*, K_2^*, where

$$K_1^* = \frac{d_2}{d_1} K_2 > 0, \quad K_2^* = \frac{d_2}{d_1} K_3 > 0,$$

with

$$K_2 = \frac{2 - \widetilde{K} - 2\sqrt{1 - \widetilde{K}}}{\widehat{K}}, \quad K_3 = \frac{2 - \widetilde{K} + 2\sqrt{1 - \widetilde{K}}}{\widehat{K}}.$$

Accordingly, it is easy to see that $\phi(K) < 0$ when $K_1^* < K < K_2^*$ and $\phi(K) > 0$ when $K > K_2^*$ or $0 < K < K_1^*$. Recalling the fact that $\min_{k \in \mathbb{N}_0 \{0\}} D_k(K) := -\phi(K)$, then if $K_1^* < K < K_2^*$ is satisfied, one has $D_k(K) > 0$ for any $k \in \mathbb{N}_0 \backslash \{0\}$; moreover, if $K > K_2^*$ or $0 < K < K_1^*$, then we have $D_k(K) < 0$ for some $k \in \mathbb{N}_0 \backslash \{0\}$. Because we have required $K < -\frac{d_2 \widetilde{K}}{d_1 \widehat{K}}$ and $K > -\frac{\widetilde{K}}{\widehat{K}}$, we can infer that equilibrium E_* for the general Degn-Harrison system (4) is locally asymptotically stable as $\max\left\{K_1^*, -\frac{\widetilde{K}}{\widehat{K}}\right\} < K < \min\left\{K_2^*, -\frac{d_2 \widetilde{K}}{d_1 \widehat{K}}\right\}$. However, it is not difficult to find that $K_2^* > -\frac{d_2 \widetilde{K}}{d_1 \widehat{K}}$. Accordingly, the positive equilibrium E_* is locally asymptotically stable as $\max\left\{K_1^*, -\frac{\widetilde{K}}{\widehat{K}}\right\} < K < -\frac{d_2 \widetilde{K}}{d_1 \widehat{K}}$. Therefore, we have confirmed the validity of condition (iii).

Finally, if there are some $k \in \mathbb{N}_0 \backslash \{0\}$ such that $D_k(K) < 0$ for $K > K_2^*$ or $0 < K < K_1^*$, then the positive equilibrium E_* may lose its stability. Now, if $K > K_2^*$ and we note the restriction condition $-\frac{\widetilde{K}}{\widehat{K}} < K < -\frac{d_2 \widetilde{K}}{d_1 \widehat{K}}$, we have $\max\left\{K_2^*, -\frac{\widetilde{K}}{\widehat{K}}\right\} < K < -\frac{d_2 \widetilde{K}}{d_1 \widehat{K}}$. However, this is impossible since $K_2^* > -\frac{d_2 \widetilde{K}}{d_1 \widehat{K}}$ regardless of whether $d_1 > d_2$ or $d_1 \leq d_2$. Now, if $0 < K < K_1^*$, combined with the restriction condition $-\frac{\widetilde{K}}{\widehat{K}} < K < -\frac{d_2 \widetilde{K}}{d_1 \widehat{K}}$, we obtain $-\frac{\widetilde{K}}{\widehat{K}} < K < K_1^*$ (where we employ the fact that $K_1^* < -\frac{d_2 \widetilde{K}}{d_1 \widehat{K}}$). In this case, the positive equilibrium E_* becomes unstable and Turing instability will emerge in the model (4). Hence, (iv) is correct. The proof is completed.

4 Pattern formation

In this section, we shall perform the pattern formation of the general Degn-Harrison chemical system (4) at the Turing instability region $K \in$

$\left(-\frac{\widetilde{K}}{\widehat{K}}, K_1^*\right)$, see (iv) of Theorem 3.

4.1 Pattern formation in one-dimensional domain

Firstly, let us perform the pattern formation of the general Degn-Harrison chemical system (4) at the Turing instability region in a one-dimensional space. To this end, taking the bounded domain $\Omega = (0, 25)$ and the parameters $a = 1.5, b1 = 0.5, p = 1, q = 9, s = 0.75, d_1 = 0.15$, and $d_2 = 2.15$. Then, we can obtain $E_* = (1, 1.0671), -\frac{\widetilde{K}}{\widehat{K}} = 0.75$ and $K_1^* = 0.956$. This implies that the Turing instability region is $K \in (0.75, 0.956)$. In order to find the spatial patterns of the general Degn-Harrison chemical system (4), we take $0.82 = K \in (0.75, 0.956)$, and our numerical results suggest that the general Degn-Harrison chemical system (4) admits the stripe patterns in the bounded domain $\Omega = (0, 25)$, see Fig. 3.

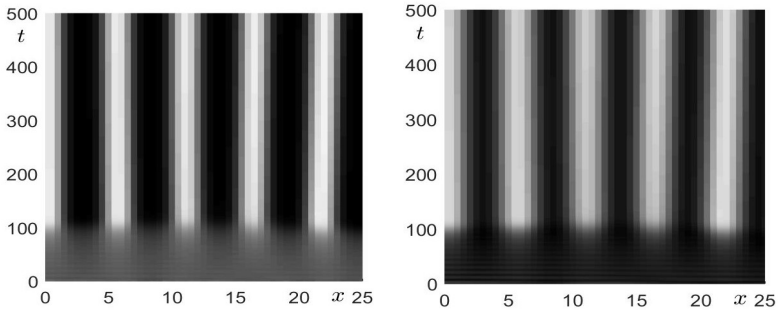

(a) $t = 500$ (b) $t = 500$

Figure 3. The general Degn-Harrison chemical system (4) admits the stripe patterns in $\Omega = (0, 25)$.

4.2 Pattern formation in two-dimensional domain

In two-dimensional space, we treat the bounded domain Ω as $\Omega = (0, 50) \times (0, 50)$. The parameters are set to $a = 2.85, b1 = 0.65, p = 1, q = 6, s = 0.25, d_1 = 0.15$, and $d_2 = 1.85$. Then, we can find $E_* = (2.2, 1.5078), -\frac{\widetilde{K}}{\widehat{K}} = 5.5604$ and $K_1^* = 5.9589$. Consequently, the Turing instability region is $K \in (5.5604, 5.9589)$. Now, we take $5.75 =$

$K \in (5.5604, 5.9589)$, we observe that the general Degn-Harrison chemical system (4) finally admits the spot patterns in the bounded domain $\Omega = (0, 50) \times (0, 50)$, see Fig. 4. Initially, irregular spatial patterns emerge in the two-dimensional bounded domain $\Omega = (0, 50) \times (0, 50)$, as shown in the first two pictures (a) and (b) in Fig. 4. However, with the reaction time t increases, spot patterns occupy the bounded region, as seen in pictures (c) and (d) in Fig. 4.

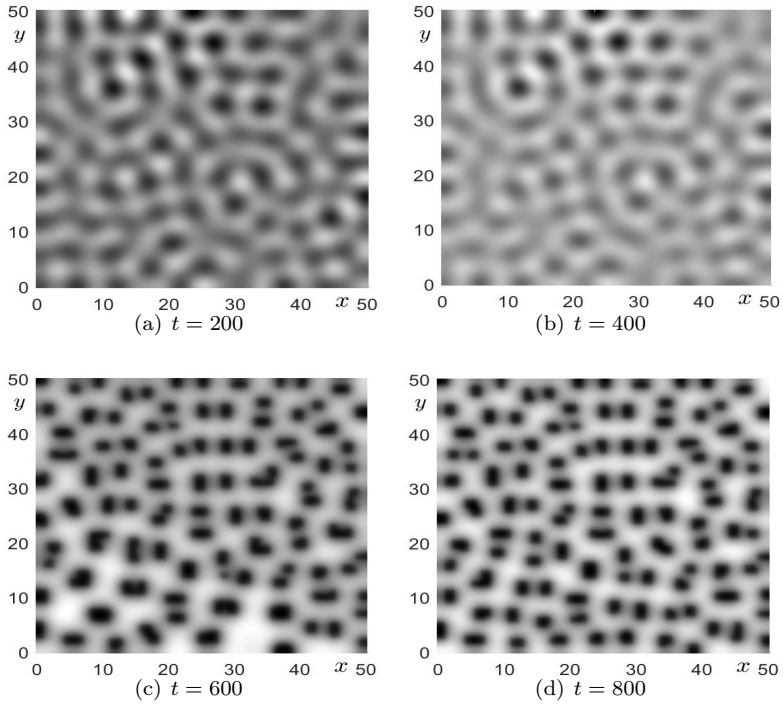

Figure 4. The general Degn-Harrison chemical system (4) admits the spot patterns in $\Omega = (0, 50) \times (0, 50)$.

4.3 Pattern formation on the torus surface

Now, we shall perform a more complex pattern evolution of the general Degn-Harrison chemical system (4) on the torus surface. Unlike the pattern formation in a bounded domain, see Figs. 3 and 4, here we investigate

the patterns of the general Degn-Harrison chemical system (4) on the torus surface. Taking the parameter values $a = 2.85, b1 = 0.65, p = 1, q = 6, s = 0.25, K = 5.75, d_1 = 0.15$, and $d_2 = 1.85$. Benefiting from Fig. 4 we know that the Turing instability region is $K \in (5.5604, 5.9589)$. Our numerical simulation results are exhibited in Fig. 5. Initially, the general Degn-Harrison chemical system (4) shows irregular stripe patterns on the torus surface, as seen in pictures (a) and (b). However, with the rapid increase of the time t, these irregular stripe patterns gradually disappear, see subfigure (c). As the reaction time t continues to increase, the irregular stripe patterns completely disappear, and the spot patterns begin to emerge on the torus surface, see picture (d). Finally, the spot patterns occupy all torus surfaces with the development of the reaction time t, see the last two pictures in Fig. 5.

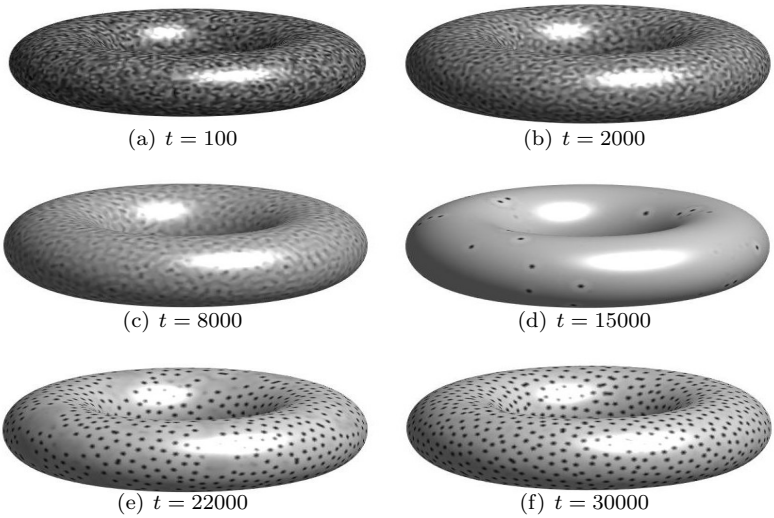

(a) $t = 100$ (b) $t = 2000$

(c) $t = 8000$ (d) $t = 15000$

(e) $t = 22000$ (f) $t = 30000$

Figure 5. The general Degn-Harrison chemical system (4) admits the spot patterns on the torus surface.

4.4 Pattern formation on the spherical surface

Figure 5 shows the pattern formation of the general Degn-Harrison chemical system (4) on the torus surface. This motivates us to explore the

pattern formation of the general Degn-Harrison chemical system (4) on the spherical surface. To this end, we keep the same parameter values in Fig. 5 while carrying out the numerical experiments on a spherical surface. Our numerical result has been performed in Fig. 6. On the spherical surface, the pattern formation is very similar to the process on the torus surface. This is because we fix $K = 5.75$ in the Turing instability domain. It is also evident that the irregular stripe patterns initially emerge on the spherical surface. However, this status is transient since the spot pattern will eventually occupy all spherical surfaces.

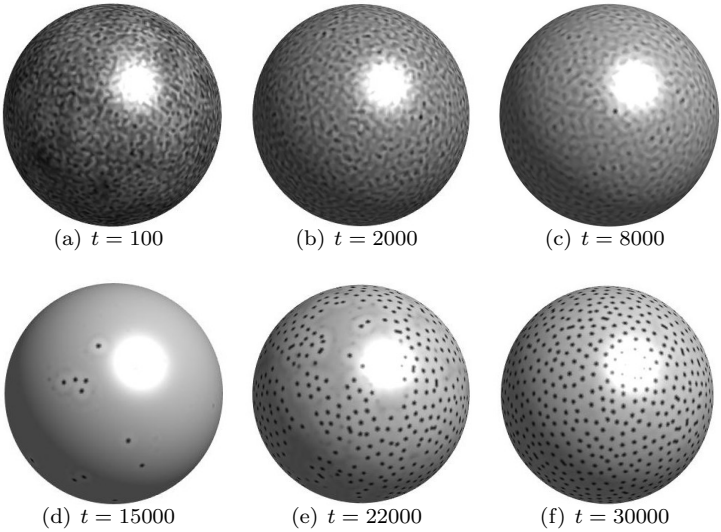

(a) $t = 100$ (b) $t = 2000$ (c) $t = 8000$

(d) $t = 15000$ (e) $t = 22000$ (f) $t = 30000$

Figure 6. The general Degn-Harrison chemical system (4) admits the spot patterns on the spherical surface.

4.5 Large diffusion rate of u inhibits pattern formation

Figures 3-6 show the spatial pattern formation of the general Degn-Harrison chemical system (4) with different parameters. It is not difficult to see that one of the necessary conditions is that the diffusion rate d_2 of the reactant v must be greater than the diffusion rate d_1 of the reactant u. In fact, for the occurrence of the patterns, d_1 is small, see Figs. 3-6. This

reminds us, is there pattern formation in the reaction-diffusion chemical system (4) as $d_2 < d_1$? To answer this question, we keep the parameters $a = 2.85, b1 = 0.65, p = 1, q = 6, s = 0.25, K = 5.75$, and $d_2 = 1.85$ as in Fig. 5 (also in Figs. 4, 6), while changing the value of d_1. First of all, one treats $d_1 = 0.15$, then we find that spot patterns on the spherical surface, as shown in Fig. 7(a). However, when we choose $d_1 = 2.5$ and $d_1 = 6.5$, all spot patterns disappear clearly, and there is no spatial pattern occupying the spherical surface, see (b) and (c) of Fig. 7. This indicates that the general Degn-Harrison chemical system (4) undergoes a state change from spatially inhomogeneous to spatially homogeneous. Namely, rapid diffusion of the reactant u will destroy the phenomenon of spatial pattern self-organization. Therefore, a large diffusion rate of u inhibits pattern formation when the diffusion rate of reactant v is fixed.

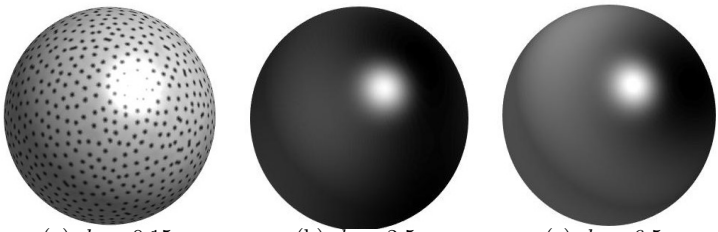

(a) $d_1 = 0.15$ (b) $d_1 = 2.5$ (c) $d_1 = 6.5$

Figure 7. Large diffusion rate of u inhibit pattern formation as diffusion rate of reactant v is fixed.

5 Conclusions

This paper considers the pattern dynamic profiles of a general chemical Degn-Harrison system. This system involves a general nonlinear reaction term $\frac{u^p v}{1+su^q}$, where $p, q > 0$. By investigating the range of the control parameters p and q, we perform the stability analysis of the unique positive equilibrium E_*. We can show that it is a node, focus, or center with the change of p and q, see Theorem 1. Note that if the equilibrium E_* is a center, then the local system (5) will undergo the Hopf bifurcation. Also, we give the direction of the Hopf bifurcation by computing the first

Lyapunov number L_1. To be precise, the Hopf bifurcation is supercritical when $L_1 < 0$ and subcritical when $L_1 > 0$ according to Theorem 2. Furthermore, we focus on the existence of Turing instability for the diffusive system (4). The rigorous theoretical predictions show that it is possible that system (4) admits the Turing instability, see Theorem 3. Based on Theorem 3, we numerically display the pattern formation of the system (4). It is shown that complex patterns can be formed in one and two-dimensional domains, on torus and spherical surfaces, as shown in Figs. 3-7. Overall, our results suggest that this chemical system could exhibit complex dynamic profiles with the general nonlinear reaction term.

***Acknowledgment*:** The authors are grateful to the anonymous referees for their helpful comments and valuable suggestions which have improved the presentation of the manuscript. This work was supported by the China Postdoctoral Science Foundation (No. 2021M701118).

References

[1] Z. X. Li, Y. L. Song, C. F. Wu, Turing instability and Hopf bifurcation of a spatially discretized diffusive Brusselator model with zero-flux boundary conditions, *Nonlin. Dyn.* **111** (2023) 713–731.

[2] M. X. Chen, R. C. Wu, B. Liu, et al., Turing-Turing and Turing-Hopf bifurcations in a general diffusive Brusselator model, *ZAMM-Z. Ang. Math. Mech.* **103** (2023) #e201900111.

[3] L. Y. Guo, X. L. Shi, J. D. Cao, Turing patterns of Gierer-Meinhardt model on complex networks, *Nonlin. Dyn.* **105** (2021) 899–909.

[4] R. Asheghi, Hopf bifurcation analysis in a Gierer-Meinhardt activator-inhibitor model, *Int. J. Bifur. Chaos* **32** (2022) #2250132.

[5] M. Gentile, I. Torcicollo, Nonlin. stability analysis of a chemical reaction-diffusion system, *Ricer. Mat.* **73** (2024) 189–200.

[6] K. Noufaey, Stability analysis for Selkov-Schnakenberg reaction-diffusion system, *Open Math.* **19** (2021) 46–62.

[7] S. B. Li, J. H. Wu, Y. Y. Dong, Turing patterns in a reaction-diffusion model with the Degn-Harrison reaction scheme, *J. Diff. Eq.* **259** (2015) 1990–2029.

[8] H. Degn, D. E. F. Harrisson, Theory of oscillations of respiration rate in continuous culture of klebsiella aerogenes, *J. Theor. Biol.* **22** (1969) 238–248.

[9] Q. Dina, U. Saeed, Stability, discretization, and bifurcation analysis for a chemical reaction system, *MATCH Commun. Math. Comput. Chem.* **90** (2023) 151–174.

[10] R. Peng, F. Q. Yi, X. Q. Zhao, Spatiotemporal patterns in a reaction-diffusion model with the Degn-Harrison reaction scheme, *J. Diff. Eq.* **254** (2013) 2465–2498.

[11] A. Abbad, S. Bendoukha, S. Abdelmalek, On the local and global asymptotic stability of the Degn-Harrison reaction-diffusion model, *Math. Meth. Appl. Sci.* **42** (2019) 567–577.

[12] B. Lisena, Some global results for the Degn-Harrison system with diffusion, *Mediterr. J. Math.* **14** (2017) #91.

[13] X.-P. Yan, J. Y. Chen, C.-H. Zhang, Dynamics analysis of a chemical reaction-diffusion model subject to Degn-Harrison reaction scheme, *Nonlin. Anal. RWA* **48** (2019) 161–181

[14] J. Zhou, Pattern formation in a general Degn-Harrison reaction model, *Bull. Korean Math. Soc.* **54** (2017) 655–666.

[15] M. X. Chen, R. C. Wu, Dynamics of a harvested predator-prey model with predator-taxis, *Bull. Malay. Math. Sci. Soc.* **46** (2023) #76.

[16] K. Manna, M. Banerjee, Spatiotemporal pattern formation in a prey-predator model with generalist predator, *Math. Model. Nat. Phenom.* **17** (2022) #6.

[17] X. Wang, F. Lutscher, Turing patterns in a predator-prey model with seasonality, *J. Math. Biol.* **78** (2019) 711–737.

[18] M. X. Chen, R. C. Wu, Steady state bifurcation in Previte-Hoffman model, *Int. J. Bifur. Chaos* **33** (2023) #2350020.

[19] M. R. Song, S. P. Gao, C. Liu, et al., Cross-diffusion induced Turing patterns on multiplex networks of a predator-prey model, *Chaos Solit. Fract.* **168** (2023) #113131.

[20] M. Dolnik, C. Konow, N. H. Somberg, et al., Effect of obstructions on growing Turing patterns, *Chaos* **32** (2022) #073127.

[21] P. Veeresha, The efficient fractional order based approach to analyze chemical reaction associated with pattern formation, *Chaos Solit. Fract.* **165** (2022) #112862.

[22] M. X. Chen, Hopf bifurcation and self-organization pattern of a modified Brusselator model, *MATCH Commun. Math. Comput. Chem.* **90** (2023) 581–607.

[23] R. C. Sarker, S. K. Sahani, Turing pattern dynamics in an SI epidemic model with superdiffusion, *Int. J. Bifur. Chaos* **32** (2022) #2230025.

[24] B. X. Zhang, Y. L. Cai, B. X. Wang, et al., Pattern formation in a reaction-diffusion parasite-host model, *Physica A* **525** (2019) 732–740.

[25] S. Issa, B. T. Mbopda, G. R. Kol, Diffusive pattern formations in three-species nonlinear dynamics of cancer, *Eur. Phys. J. Plus* **138** (2023) #469.

[26] L. Perko, *Differential Equations and Dynamical Systems*, Springer, New York, 2001.